Journal of Energy Chemistry 24 (2015) 441–447

Contents lists available at ScienceDirect

Journal of Energy Chemistry

journal homepage: www.elsevier.com/locate/jechem

Effect of loading on the Ni_2P/Al_2O_3 catalysts for the hydrotreating reactions

Junen Wang [a,b], Shaozhong Li [a], Jun Xu [a], Hui Chen [a], Jiangyu Yuan [a], Jianyi Shen [a,*]

[a] Laboratory of Mesoscopic Chemistry, School of Chemistry and Chemical Engineering, Nanjing University, Nanjing 210093, Jiangsu, China
[b] College of Chemistry and Materials Science, Huaibei Normal University, Huaibei 235000, Anhui, China

ARTICLE INFO

Article history:
Received 14 March 2015
Revised 13 April 2015
Accepted 30 June 2015
Available online 8 August 2015

Key words:
Supported Ni_2P
Liquid phase phosphidation
Triphenylphosphine
Microcalorimetric adsorption of CO
Hydrotreating reactions

ABSTRACT

The 80%Ni_2P/Al_2O_3 catalysts were prepared by the phosphidation of corresponding 80%Ni/Al_2O_3 with triphenylphosphine in liquid phase and compared with the 60%Ni_2P/Al_2O_3 for hydrotreating reactions. Both the 60%Ni_2P/Al_2O_3 and 80%Ni_2P/Al_2O_3 in comparison exhibited the small and uniform Ni_2P particles (6.3 and 8.4 nm, respectively), high CO uptakes (305 and 345 μmol/g, respectively) and thus high activities for the hydrotreating reactions. After the hydrotreating reactions, the small and uniform Ni_2P particles were remained, although the CO uptakes on the used 60%Ni_2P/Al_2O_3 and 80%Ni_2P/Al_2O_3 were greatly decreased (to 68 and 95 μmol/g, respectively) due to the incorporation of S into the Ni_2P surfaces. The 80%Ni_2P/Al_2O_3 was found to be significantly more active than the 60%Ni_2P/Al_2O_3 due to that the 80%Ni_2P/Al_2O_3 possessed more, and more active Ni_2P sites than the 60%Ni_2P/Al_2O_3, probably due to the less S incorporated in the 80%Ni_2P/Al_2O_3 than in the 60%Ni_2P/Al_2O_3 during the hydrotreating reactions.

1. Introduction

The transition metal phosphides were highly active for the hydrodesulphurization (HDS) and hydrodenitrogenation (HDN) reactions [1–3], in which the supported Ni_2P catalysts might be more active and stable than the traditional $NiMoS/Al_2O_3$ and $CoMoS/Al_2O_3$ catalysts [4,5], and thus might be used as the next-generation industrial catalysts for the hydrotreating reactions [5].

In industry, alumina is a preferred support since it possesses the strong mechanical strengths, high temperature resistance, appropriate pore structures and large surface areas. The supported Ni_2P catalysts were frequently prepared using the method of programmed temperature reduction (TPR) of nickel phosphate [1,6–9]. However, only the poorly dispersed Ni_2P catalysts were prepared with TPR method since it required high temperatures and more phosphates [10–13]. Recently, we phosphided a 60%Ni/Al_2O_3 catalyst by using triphenylphosphine (PPh_3) in liquid phase and prepared the 60%Ni_2P/Al_2O_3 catalyst with highly dispersed Ni_2P particles [14]. This 60%Ni_2P/Al_2O_3 catalyst adsorbed great amount of CO (305 μmol/g) and thus exhibited the high activities for the HDS of dibenzothiophene (DBT) and hydrogenation of tetralin to decalin.

In the present work, the Ni_2P/Al_2O_3 catalysts with higher Ni loadings (80wt%) were prepared and compared with the 60%Ni_2P/Al_2O_3 for the hydrotreating reactions. It was found that the 80%Ni_2P/Al_2O_3 prepared via the pre-reduction at 723 K exhibited the high surface density of Ni_2P active sites (345 μmol/g) as measured by the adsorption of CO. No higher values than 345 μmol/g were found in the literature so far for the adsorption of CO on Ni_2P. Our research suggested that the loading and reduction temperature significantly affected the reducibility and dispersion of supported Ni in the Ni/Al_2O_3 catalysts [15–20], which in turn affected the content and dispersion of supported Ni_2P in the phosphided Ni_2P/Al_2O_3 catalysts [21,22]. The 80%Ni_2P/Al_2O_3 with the higher CO uptake of 345 μmol/g exhibited the higher activities for the HDS of DBT and hydrogenation of tetralin to decalin than the 60%Ni_2P/Al_2O_3 with the relatively lower CO uptake of 305 μmol/g.

2. Experimental

2.1. Preparation of catalysts

The 80%Ni/Al_2O_3 was prepared by the co-precipitation method. The preparation procedure can be found elsewhere [23,24]. Briefly, desired amounts of nickel and aluminum nitrates were dissolved in 100 mL distilled water to form an aqueous solution and another aqueous solution was obtained by dissolved desired amount of sodium carbonate in 100 mL distilled water. The two solutions were simultaneously added dropwise into a beaker containing 200 mL distilled water at 353 K under vigorous stirring. The precipitate was washed thoroughly with deionized water. The filter cake was added into

* Corresponding author. Tel.: +86 25 83594305; Fax: +86 25 83594305
E-mail address: jyshen@nju.edu.cn (J. Shen).

http://dx.doi.org/10.1016/j.jechem.2015.06.014
2095-4956/

200 ml n-butanol which was then evaporated at 353 K. The sample was further dried in an oven at 393 K for 12 h.

The same phosphidation procedure was used as reported previously [22]. Typically, the 80%Ni/Al_2O_3 catalyst was placed in a micro-reactor and pre-reduced in flowing H_2 (0.1 MPa and 40 mL/min) for 2 h at different temperatures (673–823 K). Then, the temperature was lowered to 443 K, at which the catalyst was phosphided with PPh_3 (2% in heptane) for 36 h (LHSV of 2 h^{-1} and H_2/oil of 300 v/v). After the phosphidation, the catalyst was heat-treated in H_2 at 673 K for 3 h and then cooled down to the first reaction temperature (513 K), at which model diesel was introduced into the reactor and the hydrotreating reactions began.

2.2. Characterization of catalysts

The adsorption of H_2 and O_2 on the 80%Ni/Al_2O_3 catalyst was carried out in a home-made volumetric apparatus. The catalyst was reduced in H_2 at different temperatures for 2 h and evacuated at the reduction temperature for 1 h before the measurements. The adsorption of H_2 was performed at room temperature. After the adsorption of H_2, the sample was heated to 673 K at a rate of 10 K/min and evacuated at 673 K for 1 h. The adsorption of O_2 was then performed at 673 K. The uptakes of H_2 and O_2 were obtained by extrapolating the coverage of corresponding isotherms to $P = 0$. The degree of reduction (reducibility), dispersion, active surface area and average particle size of supported nickel were calculated based on the amounts of H_2 and O_2 adsorbed and the amount of nickel loaded. The detailed calculation formulae can be found in the literature [23].

The 80%Ni_2P/Al_2O_3 catalysts were prepared separately for characterizations. The phosphidation process was the same as that described above (Section 2.1). The phosphided catalysts were passivated for 12 h at room temperature under N_2 containing about 0.5 vol% O_2 before they were characterized with different techniques.

The surface area and pore structure were determined with a Micromeritics Gemini V 2380 autosorption analyzer at 77.3 K after the samples were degassed in flowing N_2 at 473 K for 5 h. X-ray diffraction (XRD) patterns were collected on a Shimadzu XRD-6000 powder diffractometer (Japan) using a Cu Kα radiation ($\lambda = 0.1541$ nm) under the setting conditions of 40 kV and 30 mA. The chemical compositions of catalysts were determined by an ARL-9800 X-ray fluorescence spectrometer (XRF). The morphologies of catalysts were performed on a JEOL JEM-2100 transmission electron microscope (TEM) operated at 200 kV.

The microcalorimetric adsorption of CO was performed by using a Setaram Tian-Calvet C-80 heat-flux microcalorimeter, connected to a gas-handling system equipped with a Baratron capacitance manometer for precise pressure measurements. Passivated samples were re-reduced in H_2 at 673 K for 3 h and then evacuated at 673 K for 1 h. The microcalorimetric adsorption was performed at 308 K.

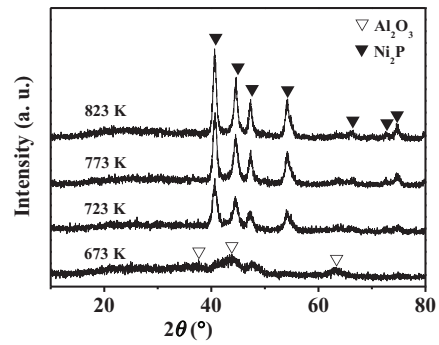

Fig. 1. XRD patterns for the 80%Ni/Al_2O_3 catalysts phosphided at 443 K with PPh_3 in liquid phase after the catalysts were pre-reduced in H_2 for 2 h at different temperatures indicated.

2.3. Catalytic tests

The reactions of HDS of DBT, HDN of quinoline and hydrogenation of tetralin were performed in a fix-bed reactor using a feed containing 1.72% DBT (3000 ppm S), 0.185% quinoline (200 ppm N), 5% tetralin and 0.5% n-octane (as an internal standard) in balanced n-tetradecane (solvent) at different temperatures (513–613 K) with the fixed pressure (3.1 MPa), LHSV (2 h^{-1}) and H_2/oil ratio (1500 (v/v)). The products were collected after 24 h and analyzed on gas chromatographs.

3. Results and discussion

3.1. Structural and surface properties of fresh catalysts

The 80%Ni/Al_2O_3 catalyst was pre-reduced at different temperatures (673–823 K) and then phosphided with PPh_3 in heptane at 443 K. Fig. 1 shows the XRD patterns of phosphided samples. When the sample was pre-reduced at 673 K, the diffraction peaks for Ni_2P were not clear. When the sample was pre-reduced at 723 K, the diffraction peaks around 40.7°, 44.6°, 47.4° and 54.2° for Ni_2P were clearly seen. The intensities of these diffraction peaks were increased with the further increase of pre-reduction temperatures to 773 and 823 K.

According to the broadening of the Ni_2P (111) peak at 40.7° and the Scherrer equation, the average particle sizes of Ni_2P formed in the 80%Ni_2P/Al_2O_3 catalysts pre-reduced at different temperatures were estimated. Table 1 shows the results. It is seen that the particle size of Ni_2P were 8.4 nm in the 80%Ni_2P/Al_2O_3 pre-reduced at 723 K. When the pre-reduction temperature was increased to 773 and 823 K, the particles of Ni_2P were correspondently increased to 10.5 and 11.9 nm, respectively. The average particle sizes of Ni_2P

Table 1
Textural and structural properties of the 60%Ni_2P/Al_2O_3 and 80%Ni_2P/Al_2O_3 catalysts phosphided at 443 K with PPh_3 in liquid phase after the 60%Ni/Al_2O_3 and 80%Ni/Al_2O_3 were pre-reduced in H_2 for 2 h at different temperatures.

Catalyst	60%Ni_2P/Al_2O_3				80%Ni_2P/Al_2O_3			
Pre-reduction temperature (K)	673	723	773	823	673	723	773	823
S_{BET} (m^2/g)	201	154	148	146	158	138	132	111
Pore volume (cm^3/g)	0.64	0.68	0.61	0.61	0.71	0.69	0.72	0.62
Pore size (nm)	9.9	13.4	12.7	13.1	15.3	15.7	17.1	17.0
XRD phase	Ni_2P	Ni_2P	Ni_2P	Ni_2P	Ni_2P	Ni_2P	Ni_2P	Ni_2P
d (nm)	4.1	6.3	6.6	7.2	–	8.4	10.5	11.9
CO uptake (μmol/g)	133	305	251	189	334	345	322	298
CO ads. heat (kJ/mol)	86	95	98	81	96	89	91	93

Note: The particle size (d) of Ni_2P was estimated by the Scherrer equation according to the full width at half maximum (FWHM) of the peak at 40.7° in the XRD patterns shown in Fig. 1.

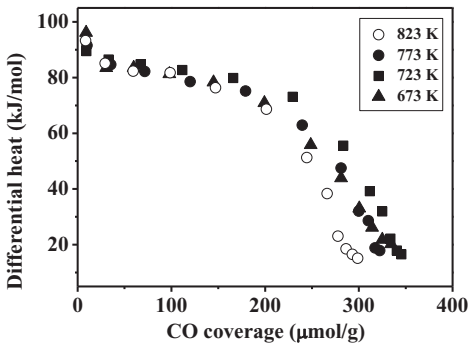

Fig. 2. Differential heats vs. coverage for CO adsorption at 308 K on the 80%Ni_2P/Al_2O_3 catalysts phosphided at 443 K with PPh_3 in liquid phase after the 80%Ni/Al_2O_3 were pre-reduced in H_2 for 2 h at different temperatures indicated. Before the adsorptions, the samples were re-reduced at 673 K in H_2 for 3 h, followed by the evacuation at 673 K for 1 h.

formed in the 60%Ni_2P/Al_2O_3 catalysts pre-reduced at different temperatures were also shown in Table 1 for comparison. Apparently, the particles of Ni_2P in the 80%Ni_2P/Al_2O_3 were significantly larger than those in the 60%Ni_2P/Al_2O_3 prepared via the same pre-reduction temperature.

Table 1 also lists the information about the surface area, pore parameters, phosphide phase, CO coverage and CO adsorption heat for the 60%Ni_2P/Al_2O_3 and 80%Ni_2P/Al_2O_3 catalysts pre-reduced at different temperatures. When the pre-reduction temperature was increased from 673 to 723 K, the surface areas were decreased from 158 to 138 m^2/g for the 80%Ni_2P/Al_2O_3 and from 201 to 154 m^2/g for the 60%Ni_2P/Al_2O_3. When the pre-reduction temperature was further increased to 773 K, the changes of surface area, pore volume and pore size of the 60%Ni_2P/Al_2O_3 and 80%Ni_2P/Al_2O_3 were not significant.

The adsorption of CO was usually used to probe the number of active sites on Ni_2P surfaces [25,26]. The heat for the adsorption of CO on Ni_2P surfaces can also be measured simultaneously [21,22,27]. The results for the adsorption of CO on the 80%Ni_2P/Al_2O_3 catalysts pre-reduced at different temperatures were shown in Fig. 2. The initial heats were measured to be 96, 89, 91 and 93 kJ/mol with the saturation coverage of 334, 345, 322 and 298 μmol/g on the 80%Ni_2P/Al_2O_3 catalysts, while the initial heats were found to be 86, 95, 98 and 81 kJ/mol with the saturation coverage of 133, 305, 251 and 189 μmol/g on the 60%Ni_2P/Al_2O_3 catalysts, prepared via the pre-reduction at 673, 723, 773 and 823 K, respectively. Apparently, the CO uptake was significantly higher on the 80%Ni_2P/Al_2O_3 than on the 60%Ni_2P/Al_2O_3 prepared with the same pre-reduction temperature.

The active Ni surface areas (or H_2 uptakes) for the Ni/Al_2O_3 catalysts were decided by the loading, reducibility and dispersion of supported Ni. The corresponding data for the 60%Ni/Al_2O_3 and 80%Ni/Al_2O_3 catalysts were compared in Table 2. It is seen that nickel in the two catalysts was not completely reduced at all the reduction temperatures from 673 to 823 K. Increase of loading of Ni increased the reducibility of Ni, but decreased the dispersion of Ni. Increase of reduction temperature also increased the reducibility of Ni, but decreased the dispersion of Ni. After the phosphidation, the CO uptakes which were used to measure the number of active sites on Ni_2P were decided by the content and dispersion of Ni_2P in the catalysts. Although we could not measure the content of Ni_2P currently, the effect of Ni content and reduction temperature on the content and dispersion of Ni_2P was clear. Apparently, the increase of loading of Ni and pre-reduction temperature increased the Ni_2P content but decreased the dispersion of Ni_2P in the resulted Ni_2P/Al_2O_3 catalysts.

From the data in Table 1, it is seen that CO uptakes on the 60%Ni_2P/Al_2O_3 changed significantly with the pre-reduction temperature, indicating that the content and dispersion of Ni_2P in the 60%Ni_2P/Al_2O_3 were strongly affected by the pre-reduction temperature. When the pre-reduction temperature increased from 673 to 723 K, the increased content of Ni_2P was more than the decreased dispersion of Ni_2P, leading to the significant increase of CO uptake. When the pre-reduction temperature increased further from 723 to 823 K, the decreased dispersion of Ni_2P was more than the increased content of Ni_2P, leading to the decrease of CO uptakes.

The effect of pre-reduction temperature on the content and dispersion of Ni_2P was smaller in the 80%Ni_2P/Al_2O_3 than in the 60%Ni_2P/Al_2O_3. This was because the 80%Ni_2P/Al_2O_3 possessed the higher loading of nickel and larger particle sizes of Ni_2P. Thus, the CO uptakes on the 80%Ni_2P/Al_2O_3 were not significantly affected by the pre-reduction temperature (see Table 1).

The presence of significant amount of unreduced Ni^{2+} in the Ni_2P/Al_2O_3 catalysts could be expected according to the data in Table 2. These unreduced Ni^{2+} cations might affect the activity of hydrotreating reactions, since they might react with H_2S formed during the hydrotreating reactions to form nickel sulfides. In fact, the used 60%Ni_2P/Al_2O_3 contained more S than the used 80%Ni_2P/Al_2O_3, which might be due to that the 60%Ni_2P/Al_2O_3 contained more unreduced Ni^{2+} than the 80%Ni_2P/Al_2O_3.

Since the 60%Ni_2P/Al_2O_3 and 80%Ni_2P/Al_2O_3 prepared via the pre-reduction at 723 K exhibited the highest CO uptakes in the respective series, they were the only two catalysts compared below.

3.2. Morphology of catalysts

Fig. 3 shows the TEM images of the reduced 80%Ni/Al_2O_3, and the fresh and used 80%Ni_2P/Al_2O_3 catalysts. It is seen that metallic Ni particles were well dispersed in the 80%Ni/Al_2O_3. The average size of Ni particles in the 80%Ni/Al_2O_3 was estimated to be about 5.5 nm, consistent with that (4.6 nm) estimated by the uptakes of H_2 and O_2. After the phosphidation at 443 K, the highly dispersed Ni_2P particles were formed in the fresh 80%Ni_2P/Al_2O_3 with the statistically averaged particle size of about 8.8 nm, consistent with that (8.4 nm) estimated by the Scherrer equation. After the hydrotreating reactions at the temperatures from 513 to 613 K, the Ni_2P particles were still highly and homogeneously dispersed in the used 80%Ni_2P/Al_2O_3

Table 2
Dispersion and reducibility of supported Ni in the 60%Ni/Al_2O_3 and 80%Ni/Al_2O_3 catalysts pre-reduced in H_2 at different temperatures.

Catalysts	60%Ni/Al_2O_3				80%Ni/Al_2O_3			
Pre-reduction temp. (K)	673	723	773	823	673	723	773	823
H_2 adsorption (μmol/g)	801	865	928	824	846	1017	947	799
O_2 adsorption (μmol/g)	2267	2906	3437	3710	3795	4649	4818	5050
Ni surface area (m^2/g)	63	68	73	65	66.2	79.6	74.1	62.6
d (nm)	2.9	3.4	3.7	4.6	4.5	4.6	5.1	8.6
Reducibility (%)	51.6	66.2	78.2	84.5	67.8	83.1	86.1	90.8
Dispersion (%)	35.3	29.8	27.0	22.2	22.3	21.9	19.7	15.8

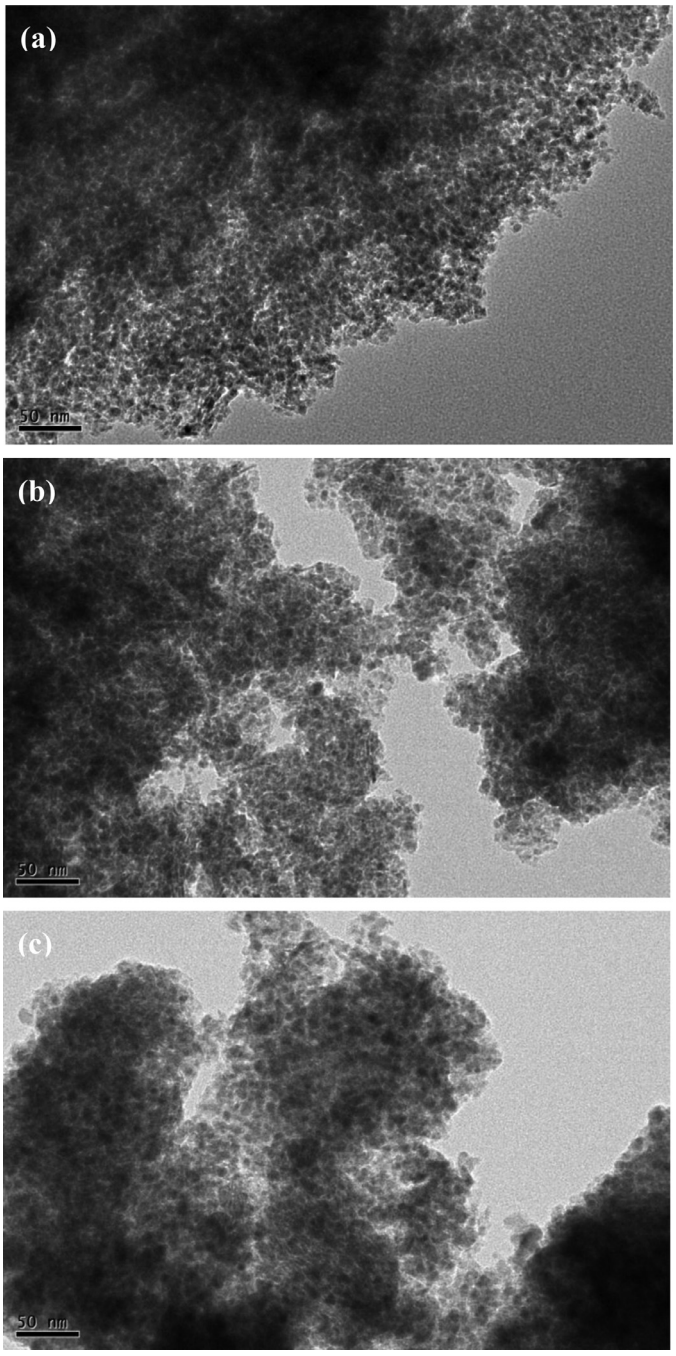

Fig. 3. TEM images of the 80%Ni/Al_2O_3 (a) fresh 80%Ni_2P/Al_2O_3 (b) and used 80%Ni_2P/Al_2O_3 (c) catalysts.

with the average size of about 9.0 nm. As compared with the average size of Ni_2P particles in the fresh 80%Ni_2P/Al_2O_3, the increase of size of Ni_2P particles during the hydrotreating reactions was not significant.

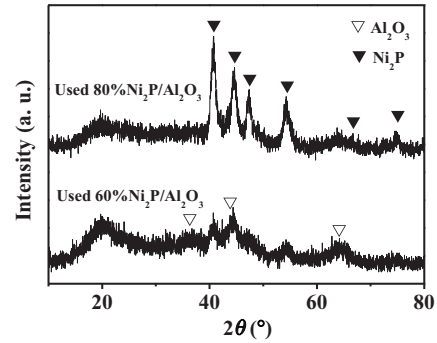

Fig. 4. XRD patterns for the used 60%Ni_2P/Al_2O_3 and 80%Ni_2P/Al_2O_3 catalysts. Reaction conditions: T = 513–613 K, P = 3.1 MPa, LHSV = 2 h^{-1} and H_2/oil = 1500 (v/v).

3.3. Structural and surface properties of used catalysts

Fig. 4 shows the XRD patterns of the used 60%Ni_2P/Al_2O_3 [14] and 80%Ni_2P/Al_2O_3 catalysts after the hydrotreating reactions. Ni_2P was the only phase detected besides Al_2O_3, indicating that Ni_2P was highly stable during the hydrotreating reactions at the reaction temperatures from 513 to 613 K. No nickel sulfide phase was detected by XRD in the used catalysts although the studies showed that S would be incorporated into the Ni_2P surfaces during the hydrotreating reactions [28,29]. According to the broadening of Ni_2P (111) peak at 40.7° and the Scherrer equation, the average sizes of Ni_2P particles in the used 60%Ni_2P/Al_2O_3 and 80%Ni_2P/Al_2O_3 were estimated to be about 6.9 and 9.1 nm, respectively (see Table 3). Thus, the increase of sizes of Ni_2P particles during the hydrotreating reactions was not significant, comparing the XRD results for the fresh and used catalysts.

The initial heats and saturation coverages for the adsorption of CO on the used 60%Ni_2P/Al_2O_3 and 80%Ni_2P/Al_2O_3 catalysts were listed in Table 3. The initial heats for the adsorption of CO were measured to be 62 and 64 kJ/mol on the used 60%Ni_2P/Al_2O_3 and 80%Ni_2P/Al_2O_3 with the saturation coverages of 68 and 95 μmol/g, respectively. The heats and coverages for the adsorption of CO were both significantly decreased as compared with those on the fresh catalysts. Since the sizes of Ni_2P particles increased only a little, the significant decrease of heats and coverages for the adsorption of CO must be caused by the incorporation of S into the Ni_2P surfaces. As compared with the used 60%Ni_2P/Al_2O_3, the used 80%Ni_2P/Al_2O_3 possessed the higher CO uptake and thus exhibited the higher activity for the hydrotreating reactions.

Table 3 also lists the information about the surface areas and pore parameters for the used 60%Ni_2P/Al_2O_3 and 80%Ni_2P/Al_2O_3 catalysts after the hydrotreating reactions. The surface areas of used 60%Ni_2P/Al_2O_3 and 80%Ni_2P/Al_2O_3 were about 164 and 120 m^2/g, respectively, which were not changed significantly as compared to those of the fresh ones. The pore volumes and pore sizes of used 60%Ni_2P/Al_2O_3 and 80%Ni_2P/Al_2O_3 were decreased, but not significantly, as compared to those of fresh ones (see Table 1).

Table 4 shows the chemical compositions of the 60%Ni_2P/Al_2O_3 and 80%Ni_2P/Al_2O_3 before and after the hydrotreating reactions. The P/Ni ratios were measured to be 0.43 and 0.64, respectively, in the fresh 60%Ni_2P/Al_2O_3 and 80%Ni_2P/Al_2O_3, while those were found to

Table 3
Textural and structural properties of the used 60%Ni_2P/Al_2O_3 and 80%Ni_2P/Al_2O_3 catalysts.

Used catalyst	S_{BET} (m^2/g)	Pore volume (cm^3/g)	Pore size (nm)	XRD phase	d (nm)	CO uptake (μmol/g)	CO ads. heat (kJ/mol)
60%Ni_2P/Al_2O_3	164	0.55	10.9	Ni_2P	6.9	68	62
80%Ni_2P/Al_2O_3	120	0.44	11.5	Ni_2P	9.1	95	64

Note: The particle size (d) of Ni_2P was estimated by the Scherrer equation according to the full width at half maximum (FWHM) of the peak at 40.7° in the XRD patterns shown in Fig. 4.

Table 4
Chemical compositions analyzed by XRF for the fresh and used 60%Ni_2P/Al_2O_3 and 80%Ni_2P/Al_2O_3 catalysts.

Catalyst	Ni (wt%)	P (wt%)	S (wt%)	P/Ni (atom)
60%Ni_2P/Al_2O_3	49.9	11.3	–	0.43
Used 60%Ni_2P/Al_2O_3	48.6	10.1	5.5	0.39
80%Ni_2P/Al_2O_3	58.4	19.7	–	0.64
Used 80%Ni_2P/Al_2O_3	58.2	19.9	2.1	0.65

be 0.39 and 0.65 in the used 60%Ni_2P/Al_2O_3 and 80%Ni_2P/Al_2O_3, respectively. The P/Ni ratio was decreased in the used 60%Ni_2P/Al_2O_3 while it was almost not changed in the used 80%Ni_2P/Al_2O_3. The content of S was significantly higher in the used 60%Ni_2P/Al_2O_3 (5.5 wt%) than in the 80%Ni_2P/Al_2O_3 (2.1 wt%), probably owing to that the 80%Ni_2P/Al_2O_3 contained less unreduced Ni^{2+} cations and more P as compared to the 60%Ni_2P/Al_2O_3. Thus, the 80%Ni_2P/Al_2O_3 seemed more resistant to S during the hydrotreating reactions.

The P/Ni ratio in the 60%Ni_2P/Al_2O_3 was significantly lower than the stoichiometric ratio of Ni_2P (0.5). This might be caused by unreduced Ni^{2+} in the catalyst, which might react with H_2S formed during the hydrotreating reaction to form nickel sulfides. In addition, S might be incorporated into Ni_2P surfaces to form NiP_xS_y species, which was considered as the active phase for the hydrotreating reactions [29–31]. The P/Ni ratio in the 80%Ni_2P/Al_2O_3 was higher than the stoichiometric ratio of Ni_2P (0.5). Besides the P in Ni_2P, other forms of P might deposit in the catalyst during the phosphidation, leading to the higher P/Ni ratios. Similarly, different forms of sulfur might be also present in the used 60%Ni_2P/Al_2O_3 and 80%Ni_2P/Al_2O_3 catalysts. However, not all the sulfur was present in the Ni_2P lattices as the component of active phase NiP_xS_y. In fact, the amounts of different forms of P and S in the Ni_2P catalysts and their effects on the hydrotreating reactions are the complicated issues to understand in the future.

3.4. Catalytic properties

Fig. 5(a) compares the activities of HDS of DBT over the 60%Ni_2P/Al_2O_3 and 80%Ni_2P/Al_2O_3 catalysts. The conversion of DBT increased with the increase of reaction temperature. At the temperatures higher than 593 K, the conversion of DBT was 100% over the 60%Ni_2P/Al_2O_3 and 80%Ni_2P/Al_2O_3 catalysts. The difference in the activity of HDS of DBT was apparent over the two catalysts at the lower temperatures. At 513 K, the conversion of DBT was 62.4 and 95.9%, respectively, over the 60%Ni_2P/Al_2O_3 and 80%Ni_2P/Al_2O_3, in consistence with their CO uptakes on the used catalysts (68 and 95 μmol/g, respectively).

The HDS of DBT usually undergoes through two pathways. One is the direct desulfurization pathway (DDS) with the formation of biphenyl (BP) as the desulfurization product, while another is the indirect desulfurization pathway, i.e., the one for the desulfurization after an aromatic ring in DBT is hydrogenated (HYD), with the formation of cyclohexylbenzene (CHB) as the desulfurization product. Fig. 5(b) shows the different selectivities for the HDS of DBT at different temperatures. With the increase of reaction temperature, the selectivity to BP decreased while that to CHB increased. For example, with the increase of reaction temperature from 513 to 613 K, the selectivity to BP decreased from 53.1% to 33.6% while that to CHB increased from 46.9% to 66.4%, over the 80%Ni_2P/Al_2O_3. At 513 K, the selectivity to BP was 76.8 and 53.1%, while that to CHB was 23.2 and 46.9% over the 60%Ni_2P/Al_2O_3 and 80%Ni_2P/Al_2O_3, respectively. This indicated that the 80%Ni_2P/Al_2O_3 exhibited the higher activity of HYD pathway, i.e., the higher activity for the hydrogenation of aromatic ring in DBT than the 60%Ni_2P/Al_2O_3.

Fig. 6(a) compares the 60%Ni_2P/Al_2O_3 and 80%Ni_2P/Al_2O_3 catalysts for the HDN of quinoline. The conversion of quinoline was 100%

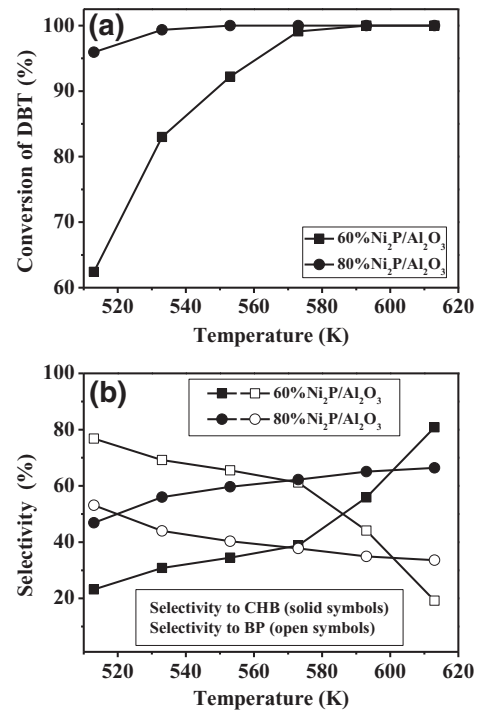

Fig. 5. Conversion of DBT (a) and selectivity to biphenyl (BP) and cyclohexylbenzene (CHB) (b) on the 60%Ni_2P/Al_2O_3 and 80%Ni_2P/Al_2O_3 catalysts. Other reaction conditions: $P = 3.1$ MPa, LHSV = 2 h^{-1} and H_2/oil = 1500 (v/v).

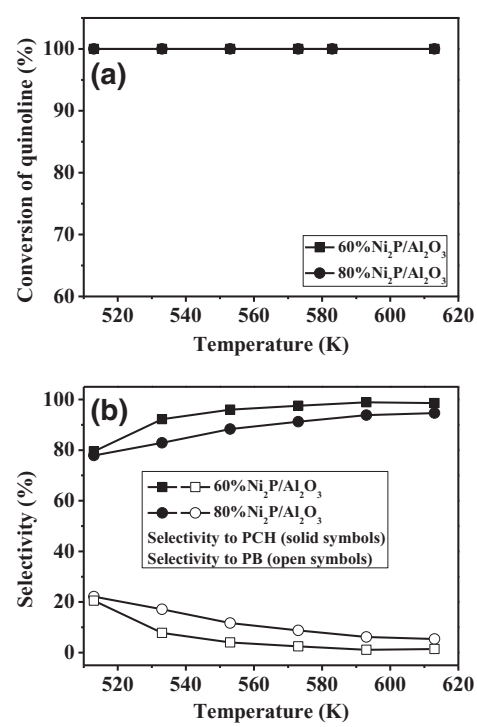

Fig. 6. Conversion of quinoline (a) and selectivity to propyl-cyclohexane (PCH) and propylbenzene (PB) (b) on the 60%Ni_2P/Al_2O_3 and 80%Ni_2P/Al_2O_3 catalysts. Other reaction conditions: $P = 3.1$ MPa, LHSV = 2 h^{-1} and H_2/oil = 1500 (v/v).

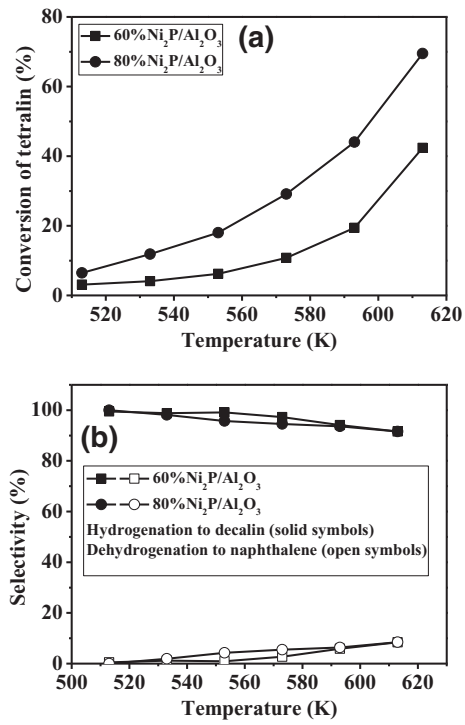

Fig. 7. Conversion of tetralin (a) and selectivity to decalin and naphthalene (b) on the 60%Ni_2P/Al_2O_3 and 80%Ni_2P/Al_2O_3 catalysts. Other reaction conditions: $P = 3.1$ MPa, LHSV = 2 h^{-1} and H_2/oil = 1500 (v/v).

over the two catalysts at the temperatures from 513 to 613 K, indicating that the difference of activity of the two catalysts for the HDN of quinoline could not be distinguished under the reaction conditions. Propylbenzene (PB) and propylcyclohexane (PCH) were the products of HDN of quinoline. The selectivities of these products are shown in Fig. 6(b). It is seen that PCH was the main product of HDN on the Ni_2P catalysts, i.e., the aromatic ring without the N atom in quinoline was easily hydrogenated on Ni_2P. In addition, the selectivity to PCH was similar over the two catalysts, but slightly higher on the 60%Ni_2P/Al_2O_3 than on the 80%Ni_2P/Al_2O_3, probably owing to that the 60%Ni_2P/Al_2O_3 contained more γ-Al_2O_3 and thus possessed stronger surface acidity [23,24].

The content of aromatic hydrocarbons in diesel fuels is an important factor determining the quality of diesel. Hydrocarbons with multi-rings have low cetane numbers and produce more particulate matters (PM) from diesel engines [32]. In this work, the hydrogenation of tetralin was used to probe the activities of Ni_2P catalysts for the hydrogenation of hydrocarbons with multiple aromatic rings. Fig. 7(a) shows the conversion of tetralin over the 60%Ni_2P/Al_2O_3 and 80%Ni_2P/Al_2O_3 catalysts at different reaction temperatures. The conversion of tetralin increased with the increase of reaction temperatures from 513 to 613 K. The conversion of tetralin was higher on the 80%Ni_2P/Al_2O_3 than on the 60%Ni_2P/Al_2O_3 at the same reaction temperatures. For example, the conversion of tetralin was determined to be 42.4 and 69.5%, respectively, at 613 K over the 60%Ni_2P/Al_2O_3 and 80%Ni_2P/Al_2O_3.

Tetralin might be hydrogenated to decalin (HYD) or dehydrogenated to naphthalene (DHYD) over the Ni_2P catalysts. Fig. 7(b) shows the selectivities to decalin and naphthalene over the 60%Ni_2P/Al_2O_3 and 80%Ni_2P/Al_2O_3 catalysts at different reaction temperatures. It is seen that decalin was the main product of hydrogenation of tetralin. With the increase of reaction temperature, the selectivity to decalin decreased while that to naphthalene increased. In addition, the selectivity to decalin was quite similar over the two catalysts.

Table 5
Turnover frequencies (TOF) of HDS of DBT and hydrogenation of tetralin on the 60%Ni_2P/Al_2O_3 and 80%Ni_2P/Al_2O_3 catalysts.

Catalyst	HDS of DBT at 513 K (10^{-4} s^{-1})	Hydrogenation of tetralin to decalin at 613 K (10^{-4} s^{-1})
60%Ni_2P/Al_2O_3	4.8	12.0
80%Ni_2P/Al_2O_3	5.2	14.1

The turnover frequencies (TOF) for the HDS of DBT and the hydrogenation of tetralin to decalin were calculated according to the CO uptakes on the used 60%Ni_2P/Al_2O_3 and 80%Ni_2P/Al_2O_3 catalysts. The results are given in Table 5. The 80%Ni_2P/Al_2O_3 exhibited the higher TOF values than the 60%Ni_2P/Al_2O_3 for the HDS of DBT and hydrogenation of tetralin to decalin, indicating that the 80%Ni_2P/Al_2O_3 had the Ni_2P sites with higher intrinsic activities, which might be associated with the lower content of S in the 80%Ni_2P/Al_2O_3 during the hydrotreating reactions.

4. Conclusions

Following conclusions can be drawn from the above results:

(1) The Ni_2P/Al_2O_3 catalysts could be prepared by the pre-reduction and then phosphidation of corresponding Ni/Al_2O_3 catalysts. It was found that the 60%Ni_2P/Al_2O_3 and 80%Ni_2P/Al_2O_3 prepared by the pre-reduction at 723 K in H_2 followed by the phosphidation at 443 K with PPh_3 in liquid phase exhibited the highest CO uptakes (305 and 345 μmol/g, respectively).

(2) The conversion of HDS of DBT was 62.4 and 95.9% at 513 K and that of hydrogenation of tetralin was 42.4 and 69.5% at 613 K over the 60%Ni_2P/Al_2O_3 and 80%Ni_2P/Al_2O_3 catalysts, respectively, indicating that the 80%Ni_2P/Al_2O_3 was significantly more active than the 60%Ni_2P/Al_2O_3 for the HDS of DBT and hydrogenation of tetralin to decalin.

(3) The XRD and TEM results showed the highly and homogeneously dispersed Ni_2P nano particles in the fresh (6.3 and 8.4 nm, respectively) and used (6.9 and 9.1 nm, respectively) 60%Ni_2P/Al_2O_3 and 80%Ni_2P/Al_2O_3 catalysts, indicating that such Ni_2P nano particles were highly stable during the hydrotreating reactions at the temperatures from 513 to 613 K.

(4) After the hydrotreating reactions, the CO uptakes on the used 60%Ni_2P/Al_2O_3 and 80%Ni_2P/Al_2O_3 catalysts were greatly decreased to 68 and 95 μmol/g, respectively, due to the incorporation of S into the Ni_2P surfaces.

(5) After the hydrotreating reactions, the used 80%Ni_2P/Al_2O_3 exhibited the higher CO uptake than the used 60%Ni_2P/Al_2O_3, indicating that the 80%Ni_2P/Al_2O_3 possessed more active sites of Ni_2P than the 60%Ni_2P/Al_2O_3 for the hydrotreating reactions. In addition, the TOF values for the HDS of DBT and hydrogenation of tetralin were significantly higher on the 80%Ni_2P/Al_2O_3 than on the 60%Ni_2P/Al_2O_3, indicating that the Ni_2P sites were more active in the 80%Ni_2P/Al_2O_3 than in the 60%Ni_2P/Al_2O_3, probably owing to the less S content in the 80%Ni_2P/Al_2O_3 than in the 60%Ni_2P/Al_2O_3. Thus, the 80%Ni_2P/Al_2O_3 seemed more resistant to S than the 60%Ni_2P/Al_2O_3 for the hydrotreating reactions.

Acknowledgments

Financial supports from NSFC (21273105), MSTC (2013AA031703), NSFJC (BK20140596) and the fundamental research funds for central universities are acknowledged.

References

[1] A. Infantes-Molina, C. Moreno-Leon, B. Pawelec, J.L.G. Fierro, E. Rodriguez-Castellon, A. Jimenez-Lopez, Appl. Catal. B: Environ. 113-114 (2012) 87.
[2] J.R. Hayes, R.H. Bowker, A.F. Gaudette, M.C. Smith, C.E. Moak, C.Y. Nam, T.K. Pratum, M.E. Bussell, J. Catal. 276 (2) (2010) 249.
[3] J.A. Cecilia, A. Infantes-Molina, E. Rodriguez-Castellon, A. Jimenez-Lopez, J Catal 263 (1) (2009) 4.
[4] X.Q. Wang, P. Clark, S.T. Oyama, J. Catal. 208 (2) (2002) 321.
[5] S.T. Oyama, J. Catal. 216 (1-2) (2003) 343.
[6] S.T. Oyama, H.Y. Zhao, H.J. Freund, K. Asakura, R. Wlodarczyk, M. Sierka, J. Catal. 285 (1) (2012) 1.
[7] V. Zuzaniuk, R. Prins, J. Catal. 219 (1) (2003) 85.
[8] S.J. Sawhill, D.C. Phillips, M.E. Bussell, J. Catal. 215 (2) (2003) 208.
[9] J. Chen, H. Shi, L. Li, K. Li, Appl. Catal. B: Environ. 144 (0) (2014) 870.
[10] P.A. Clark, S.T. Oyama, J. Catal. 218 (1) (2003) 78.
[11] S.J. Sawhill, K.A. Layman, D.R. Van Wyk, M.H. Engelhard, C. Wang, M.E. Bussell, J. Catal. 231 (2) (2005) 300.
[12] K.-S. Cho, H.-R. Seo, Y.-K. Lee, Catal. Commun. 12 (6) (2011) 470.
[13] J.A. Cecilia, A. Infantes-Molina, E. Rodriguez-Castellon, A. Jimenez-Lopez, Appl. Catal. B: Environ. 92 (1-2) (2009) 100.
[14] J. Wang, Y. Fu, H. Chen, J. Shen, *Chem Eng J* (in press).
[15] S. Narayanan, R. Unnikrishnan, V. Vishwanathan, Appl Catal A: gen 129 (1) (1995) 9.
[16] S. Narayanan, R. Unnikrishnan, Appl. Catal A: Gen 145 (1) (1996) 231.
[17] R. Molina, G. Poncelet, J. Catal. 199 (2) (2001) 162.
[18] P. Savva, K. Goundani, J. Vakros, K. Bourikas, C. Fountzoula, D. Vattis, A. Lycourghiotis, C. Kordulis, Appl. Catal. B: Environ. 79 (3) (2008) 199.
[19] S. Hu, M. Xue, H. Chen, Y. Sun, J. Shen, Chin. J. Catal. 32 (6) (2011) 917.
[20] F. Li, X. Yi, J. Zheng, H. Jin, W. Fang, Catal. Commun. 11 (4) (2009) 266.
[21] Y. Zhao, M. Xue, M. Cao, J. Shen, Appl. Catal. B: Environ. 104 (3-4) (2011) 229.
[22] J. Wang, H. Chen, Y. Fu, J. Shen, Appl. Catal. B: Environ. 160–161 (0) (2014) 344.
[23] S. Hu, M. Xue, H. Chen, J. Shen, Chem. Eng. J. 162 (1) (2010) 371.
[24] J. Zhao, H. Chen, J. Xu, J. Shen, J. Phys. Chem. C 117 (20) (2013) 10573.
[25] S.T. Oyama, Y.-K. Lee, J. Catal. 258 (2) (2008) 393.
[26] G.-N. Yun, Y.-K. Lee, Appl. Catal. B: Environ. 150 (647) (2014).
[27] Y. Zhao, Y. Zhao, H. Feng, J. Shen, J. Mater. Chem 21 (22) (2011) 8137.
[28] A.E. Nelson, M. Sun, A.S.M. Junaid, J. Catal. 241 (1) (2006) 180.
[29] S.T. Oyama, X. Wang, Y.K. Lee, W.J. Chun, J. Catal. 221 (2) (2004) 263.
[30] K.A. Layman, M.E. Bussell, J. Phys. Chem. B 108 (30) (2004) 10930.
[31] K.A. Layman, M.E. Bussell, J. Phys. Chem. B. 108 (40) (2004) 15791.
[32] M. Santikunaporn, J.E. Herrera, S. Jongpatiwut, D.E. Resasco, W.E. Alvarez, E.L. Sughrue, J. Catal. 228 (1) (2004) 100.